Equilibrium Properties of Diblock Copolymer Thin Films on a Heterogeneous, Striped Surface

G. G. Pereira*,†,‡ and D. R. M. Williams†

Department of Applied Mathematics, Research School of Physical Sciences and Engineering, Australian National University Canberra ACT, 0200 Australia, and School of Chemistry, University of Sydney, NSW 2006, Australia

Received February 18, 1998; Revised Manuscript Received May 5, 1998

ABSTRACT: Recent experiments have shown it is possible to produce striped surfaces with periodicities of the same order as those for self-organized diblock copolymer lamellae. Here we study theoretically the behavior of a thin film of AB diblocks on a CD striped surface. The competition between the preferred bulk lamellar spacing and the spacing favored by the stripes leads to several novel phases. We study this system by analytical and numerical means and in one limit by mapping it onto the Frenkel−Kontorowa model of solid state physics. The main conclusion is that the periodically striped surface can induce lamellae of unequal spacing. We also show that the surface can induce inverted bilayers where an AB is followed directly by another AB rather than a BA.

1. Introduction

Much attention has been paid in recent years to the self-assembly of AB diblock copolymers.[1−10] These consist of an A and a B homopolymer joined at one end. The immiscibility of the two blocks drives them to microphase separate into a number of different phases. For the symmetric diblocks, which we shall study here, a lamellar phase is favored with an AB followed by a BA in series. Much of the work has focused on bulk samples or on samples on homogeneous surfaces. It has recently become possible to create striped surfaces with a stripe period close to that of the bulk lamellar period.[11] Here we study theoretically what can occur when a melt of symmetric diblock copolymers is placed on such a surface. A preliminary report of some of our results has already been published.[12] Here we present a detailed study of this system, including all the free energy functionals used in calculating the phase diagram.

We assume that the bottom striped surface is flat as is the top air/polymer interface. The lower surface is treated (chemically or otherwise) to form periodic stripes of width λ. Such striped surfaces are produced from nanoscopically grooved Si[113] single-crystal wafers combined with glancing angle metal evaporation. This produces a shadowing of the surface features and results in a surface that consists of alternating stripes of silicon and evaporated metal. The technique is reproducible and can produce stripes of width comparable to the bulk equilibrium diblock copolymer spacing. Further details of this technique may be found in ref 11. These stripes can favor either the A or B parts of the diblock. In this system there is a competition between the bulk periodicity of the lamellae and the periodicity imposed by the surface. We will show that this competition leads to several interesting phase transitions. For example let us consider a CDCD striped surface with the C stripes favoring the B part of the diblock and the D stripes favoring the A part of the diblock. If the surface−diblock interfacial energy is sufficiently large, the diblocks will assemble so that the A parts completely align with the D stripes and the B parts will completely align with the C stripes. Thus the lamellar layer spacing is commensurate with the surface's stripe width. Conversely, if the surface−diblock interfacial energy is sufficiently small, the diblocks will take on a spacing close to the bulk lamellar spacing, which is not necessarily equal to λ.

While this system is obviously of interest from the point of view of polymer science, i.e., it provides a way of growing single "crystals" of diblock copolymers, there is also a motivation for our study that comes from theoretical physics. This system has certain qualitative features in common with a model from solid-state physics known as the Frenkel−Kontorowa (FK) model.[13−15] In the FK model atoms with a certain bulk separation of b units are placed on a one-dimensional periodic surface. Depending on the magnitude of the surface−atom energy, with respect to the atom−atom energy, the atoms may take on spacings commensurate with the surface's periodic spacing c units, or incommensurate with c. The system we are considering has some common qualitative features with this model. However, the two are not precisely identical. In particular, our surface induces a "square-wave" potential rather than a more weakly changing sinusoidal potential. More importantly, our system has directionality as well as position. In the bulk system (away from any surfaces) an AB lamella is followed by a BA lamella; i.e., in the language of the Ising model an "up" spin is followed by a "down" spin. This minimizes the AB interfacial energy. In a system with surface interactions this is not neccessarily the case and an AB lamella may be followed by another AB lamella. We shall call this kind of pattern, AB, AB, an inverted configuration.

In the system we are considering there are a large number of parameters. As stated above, we specialize to the case of symmetric diblocks where the chemically different A and B blocks have the same degree of polymerization and the same monomer size. With this restriction on the block sizes the bulk morphology will be a lamellar phase.[16−18] We also assume implicitly that

* To whom correspondence should be addressed.
† Australian National University.
‡ University of Sydney.

S0024-9297(98)00244-7 CCC: $15.00
Published on Web 08/08/1998

the system reaches equilibrium, i.e., that it minimizes the free energy. In real experiments the system may be trapped in local minima and long annealing times may be necessary to reach equilibrium. In this paper we assume that the lamellae are perpendicular to the surface. This implies that we consider only the case where the surface stripes have a length less than the natural lamellar spacing. In the other case where the stripe length is larger than the natural spacing, the lamellae may tilt to accommodate the surface potential. This is discussed briefly in section 3 below. In addition, we assume that the top air/copolymer interface is flat. One finds experimentally that, when the bulk lamellar spacing is not equal to the stripe width, the system is frustrated and so may undulate.[10] As this is the first theoretical study of a striped system, we consider here only the simplest morphology, i.e., a flat air/copolymer interface.

The outline of our paper is as follows. In section 2 we introduce the diblock−stripe model and evaluate its free energy for a general number of stripes. We then study two small systems with four and six stripes. This is done because these systems are readily understandable and exhibit most of the features seen in larger systems. The reader is, however, warned that these small systems also exhibit some anomolous phase behavior due to the small number of stripes. In particular they exhibit a stretched phase where two lamellae span the entire system. This obviously cannot occur for much larger systems. In section 3 we consider a larger stripe system, to which we numerically determine the phase diagram. In section 4 we discuss the connection between our diblock−stripe model to the Frenkel−Kontorowa model. Finally in section 5 we give our conclusions and a brief comparison with the preliminary experimental results.

2. Diblock−Stripe Model

Consider the free energy of a bulk melt of diblocks with lamellar spacing L_b.[18] Each diblock copolymer has $2N$ monomers each of size a. The free energy is a sum of the elastic stretching energy and surface energy at the A−B interface. The free energy per diblock is F_b and given by

$$F_b = \frac{\pi^2 k_B T}{24a^2}\frac{L^2}{2N} + \gamma_{AB}\frac{2Na^3}{L} \tag{1}$$

so that the equilibrium diblock thickness is

$$L_b = \left(\frac{48\gamma_{AB}a^5}{\pi^2 k_B T}\right)^{1/3} N^{2/3} \tag{2}$$

where γ_{AB} is the AB surface tension and T is the temperature. This is the natural lamellar spacing, i.e., the spacing in the absence of surface effects.

Now consider the diblock−surface system, where the surface is subdivided into stripes of width λ (in the x direction) and length w (in the y direction) (see Figure 1). The length w is taken later to be infinite and plays no role in the results. The z direction is normal to the surface. We assume periodic boundary conditions in the x direction so that the surface is effectively wrapped onto a cylinder. The stripes are alternating in affinity for either the A or B part of a diblock. For simplicity we shall say the surface is composed of CDCD... stripes, with equal numbers of C and D stripes. A diblock melt is then placed on the surface and allowed to reach equilibrium. The major effect of the striped surface would be expected to show on the macroscopic lamellar layer spacing of an AB diblock. If the surface−diblock potential is sufficiently large, the diblocks would be expected to assemble commensurate with the stripes. Conversely, if γ_{AB} is sufficiently large, the diblocks would be expected to assemble with the natural lamellar spacing. Usually these are competing effects, and the actual spacing can be found by minimizing the total free energy.

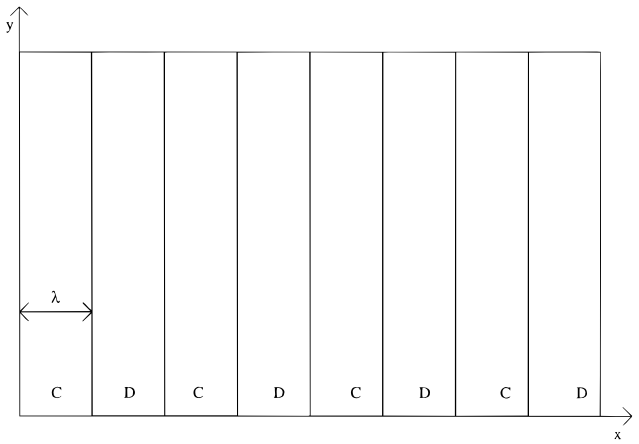

Figure 1. Schematic of the striped substrate surface. The z-axis comes out of the plane of the page.

The critical part of the study thus lies in calculating the free energy of the melt of diblocks. The free energy F of the system is the sum of elastic and interfacial energy components:

$$F = \frac{\pi^2 k_B T}{48Na^2}\sum_{i=1}^{n_l}(x_{i+1} - x_i)^2 n_i + \gamma_{AB} whn_l + \sum_{i=1}^{n_l}\gamma_{AB} wh\delta(\text{ABAB}) + F_{\text{surface-diblock}} \tag{3}$$

where n_l is the number of lamellar layers and $n_i = wh(x_{i+1} - x_i)/2Na^3$ is the number of diblocks in each lamellar layer. The total number of diblocks in the system is a constant. The thickness of the lamellar system in the z direction is h. The first term in eq 3 is the stretching free energy of the diblocks. The second term is the interfacial energy of the AB interfaces. In the absence of surfaces these are the only terms that are present. The third term in eq 3 accounts for diblocks in an inverted configuration, i.e., an AB, AB configuration. The δ function is given by

$$\delta(\text{ABAB}) = \begin{cases} 1 & \text{if } i \text{ and } i+1 \text{ form an AB, AB or BA, BA configuration} \\ 0 & \text{if } i \text{ and } i+1 \text{ form an AB, BA or BA, AB configuration} \end{cases} \tag{4}$$

The last term in eq 3 represents the interfacial energy between the diblocks and the striped surface and is the only difficult term in the free energy. Its calculation is essentially a counting problem. That is, given an initial starting point of the diblock (x_i) and an ending point

(x_{i+1}) as well as its configuration (AB or BA), we must simply determine the amount of A−C, A−D, B−C, and B−D interfacial areas. This must be done over all n_l lamellae. In counting the amounts of AC interface, AD interface, etc., we must know whether the diblocks are in an AB configuration or a BA configuration. For diblocks in an AB configuration we define F_{sdn} as the corresponding striped-surface−diblock interfacial energy given by

$$\frac{F_{sdn}}{w} = \gamma_1 l_1(x_i, x_m) + \gamma_{-1} l_1(x_m, x_{i+1}) + \gamma_s\left(\frac{x_{i+1} - x_i}{2}\right) \quad (5)$$

where $x_m \equiv (x_i + x_{i+1})/2$ and $l_1(z_1,z_2)$ represents the length of C interface between the points z_1 and z_2. The parameters γ_1, γ_{-1}, and γ_S are defined by $\gamma_1 \equiv \gamma_{AC} - \gamma_{AD}$, $\gamma_{-1} \equiv \gamma_{BC} - \gamma_{BD}$, and $\gamma_s \equiv \gamma_{AD} + \gamma_{BD}$. Here γ_{ij} is the interfacial tension between substances i and j. For a diblock in a BA configuration F_{sdr} is the corresponding striped-surface−diblock interfacial energy and is given by

$$\frac{F_{sdr}}{w} = \gamma_{-1} l_1(x_i, x_m) + \gamma_1 l_1(x_m, x_i+1) + \gamma_s\left(\frac{x_{i+1} - x_i}{2}\right) \quad (6)$$

Thus, summing over all lamellar layers, using eqs 5 and 6, we finally obtain the following expression for the total free energy per unit length of the diblock−stripe system

$$F = \frac{F}{w} = h\gamma_{AB}\left\{\frac{1}{2L_b{}^3}\sum_{i=1}^{n_l}(x_{i+1} - x_i)^3 + n_l + \sum_{i=1}^{n_l}\delta(\mathrm{ABAB})\right\} + \sum_{i=1}^{n_l}[\gamma_1 l_1(x_i, x_m) + \gamma_{-1} l_1(x_m, x_{i+1})]\zeta(\mathrm{AB}) + \sum_{i=1}^{n_l}[\gamma_{-1} l_1(x_i, x_m) + \gamma_1 l_1(x_m, x_{i+1})]\zeta(\mathrm{BA}) + \frac{\gamma_s \Omega}{2} \quad (7)$$

where $\zeta(\mathrm{AB}) = 1$ if a diblock is in the AB configuration and $\zeta(\mathrm{AB}) = 0$ if the diblock is in a BA configuration and similarly for $\zeta(\mathrm{BA})$. Ω denotes the total length of the system. In the following, to reduce the number of parameters, we consider N, b, and T to be fixed. Thus, according to eq 2, $\gamma_{AB}/L_b{}^3$ is a constant, which we denote by κ for convenience in the rest of the paper. (Note the constant κ has dimensions of energy/length^5.) Note that the last term in eq 7 is a constant so that the variable part of the free energy is only dependent on h, L_b, and, as we shall see, $\gamma_1 - \gamma_{-1}$. We further consider the case where the A blocks prefer the D stripes and the B blocks the C stripes so that $\Delta\gamma = \gamma_1 - \gamma_{-1} > 0$. The reverse situation follows by symmetry.

In this calculation we have totally ignored the effects of the top surface, i.e., the air/polymer interface. Provided this surface is flat and the lamellae remain perpendicular to the striped surface, the free energy of the top surface is a constant, independent of the x_i's and the orientation of the lamellae (i.e., AB, AB or AB, BA). If we allow the top surface to undulate or if we considered lamellae parallel to the striped surface, the interfacial energy of the top surface would play an important role.

2.1. Four-Stripe Model. Experimentally, the systems of interest will have many stripes. Such a system is difficult to analyze analytically or numerically. For this reason, and as an introduction to the physics of the system, we first consider cases where there are a very small number of stripes. In real experimental systems this limitation to small numbers of stripes may also be relevant because the diblocks may reach only local equilibrium with only a few stripes being involved.

We now consider the simplest possible model that will produce any interesting behavior. The smallest number of stripes is obviously 2. However, such a system does not show any interesting behavior because only one configuration can exist, that being a lamellar layer of spacing 2λ with A and B parts of the diblock aligned depending on which part is preferred by the C stripe and which part is preferred by the D stripe. Consequently, we initially consider a four stripe system, with two C and two D stripes.

We have first studied this model numerically using a brute force minimization of the free energy eq 7 discussed below in section 3. This numerical study showed the existence of only two equilibrium phases, which we call the surface phase and the stretched phase. In principle there are at least five possible equilibrium configurations that may exist in this system. These are (i) a surface phase with four equal lamellae of spacing λ, (ii) a surface phase with four equal lamellae of spacing λ (this configuration is different from (i) since the lamellae are stacked in an inverted configuration, i.e., AB, AB instead of AB, BA), (iii) a stretched phase with two equal lamellae of spacing 2λ, (iv) a stretched phase with equal lamellae of spacing 2λ (this configuration is different from (iii) because the diblocks form the pattern AB, BA whereas in (iii) we only have AB), (v) a situation where we have more lamellae than stripes. We initially discuss these five configurations (see Figure 2). In the first two configurations in Figure 2 the diblocks completely align with the striped surface potential, i.e., A with D and B with C. If one were to simply look at these two configurations, there would be no observable difference. The difference lies in the fact that in (i) the diblocks are stretched less, i.e., only through a distance λ compared to (ii) where the diblocks are stretched through a distance 2λ. As far as free energies are concerned, (i) will be favored over (ii), since although both configurations have the same interfacial energies, (i) has lower stretching energy. Figure 2(iii) and (iv) represent the situation where the γ_{AB} interfacial tension is dominant and so as few as possible AB interfaces should appear. Due to the fact that we have periodic boundary conditions the minimum number of AB interfaces is 2. Once again, although (iii) and (iv) show no observable difference and have the same interfacial energies, (iv) is favored over (iii) due to the fact that it has a lower stretching energy. Finally, in Figure 2(v) we show a situation where more than four lamella layers appear in the system. This configuration will never have the lowest free energy because for $L_b \geq \lambda$ it will never be able to obtain its natural spacing, i.e., L_b, and also it will never be able to minimize the surface−diblock potential, as does configuration (i).

Thus there are only two phases that actually appear in this system. They are a "surface" phase with a lamellar spacing of λ, where the A parts align with D

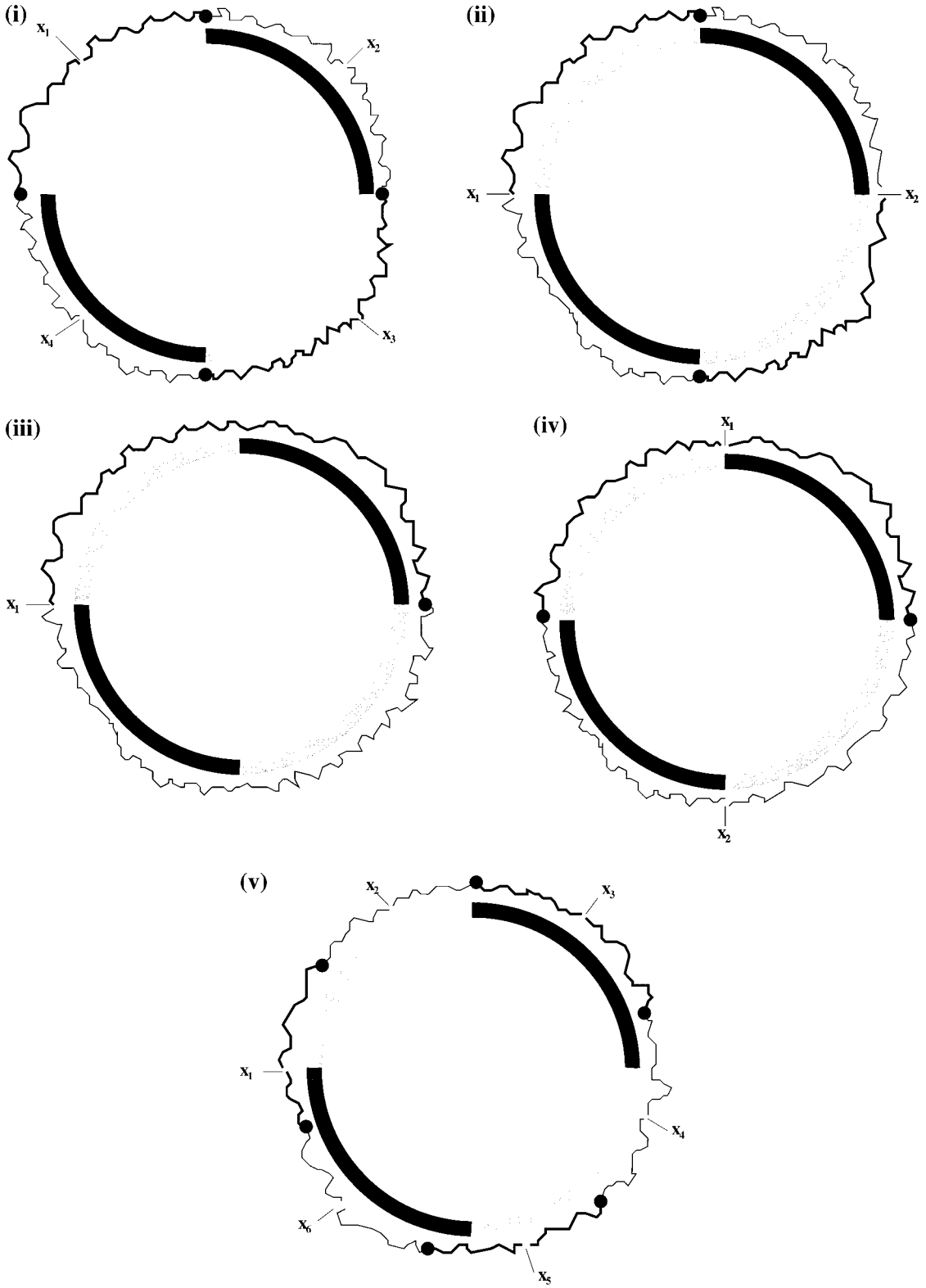

Figure 2. Five possible configurations that may occur in the four-stripe model. The thick gray stripes represents the C stripes, the thick black stripes represent D stripes. Polymers are represented by wiggly lines, the A blocks are represented by the thinner lines, and thicker lines represent the B blocks. The black dots represent where the A and B blocks have been terminally attached. In (i) and (ii) the lamellae are aligned such that they minimize the surface−diblock potential. In (iii) and (iv) the lamellae are arranged so that they minimize the number of AB interfaces. In (v) we show a situation where there are more lamellae than stripes, i.e., six AB lamellae and four stripes.

stripes and B parts align with C stripes, Figure 2(i). The second phase that can exist we shall call a "stretched" phase and corresponds to a system where the minimum possible number of AB interfaces appears, Figure 2(iv). This stretched phase, in the terminology of the FK model, is a floating phase because it appears independently of the surface potential and so has x_i's anywhere with respect to C and D stripes.

The free energy of the surface phase is F_{surf} and is given by

$$F_{surf} = h\gamma_{AB}\left[\frac{2\lambda^3}{L_b^3} + 4\right] + 2\lambda[\gamma_{AD} + \gamma_{BC}] \qquad (8)$$

To determine the free energy of the stretched phase, we note that the A and B parts of the diblock must have equal length and share the same amount of C and D interfaces. Thus the free energy of the stretched phase $F_{stretch}$ is

$$F_{stretch} = h\gamma_{AB}\left[\frac{8\lambda^3}{L_b^3} + 2\right] + \lambda[\gamma_{AC} + \gamma_{AD} + \gamma_{BC} + \gamma_{BD}] \qquad (9)$$

Now for any particular values of the parameters h, γ_{AB}, and the surface−diblock interfacial energies we may either have the surface or the stretched phase appearing in the system. Which phase does appear depends on which of these configurations corresponds to the minimum free energy. Thus we define $\Delta F \equiv F_{stretch} - F_{surf}$ so that

$$\Delta F = h\gamma_{AB}\left[\frac{6\lambda^3}{L_b^3} - 2\right] + \lambda(\gamma_1 - \gamma_{-1}) \qquad (10)$$

In this expression the only parameters that appear are h, γ_{AB}, L_b and $\Delta\gamma = \gamma_1 - \gamma_{-1}$. Furthermore, the surface−diblock interfacial energies only appear through $\Delta\gamma$, which is positive, corresponding to the assumption we have made above regarding affinity of stripes and diblocks. If ΔF is positive, this implies the phase that appears in the system will be the surface phase while if ΔF is negative the phase that appears will be the stretched phase. At $\Delta F = 0$ there is a phase transition from the surface to stretched phase. This transition is first-order since the lamellar layer's equilibrium spacing changes discontinuously from λ to 2λ.

We can now draw the phase diagram for the system. The phase diagram is a function of three dimensionless variables given by $G \equiv \Delta\gamma/\kappa\lambda^3$, $H \equiv h/\lambda$, and $L \equiv L_b/\lambda$. For a given L the phase transition occurs on a line in the $H-G$ plane. This critical line is then given by solving $\Delta F = 0$ i.e.,

$$H_c = \frac{G}{[2L^3 - 3]} \qquad \text{for} \qquad L > 3^{1/3} \qquad (11)$$

Figure 3 shows the phase diagram for this system in the $H-G$ plane for a particular value of L such that $L > 3^{1/3}$.

The physics of this diagram is clear. At fixed surface tensions (i.e., G fixed), if we increase the thickness of the film, the surface should become less and less important. Thus as we climb the H axis, we go from a surface phase to a stretched phase.

As L increases, the denominator in eq 11increases. Thus the gradient of the critical line decreases and the region of the phase diagram corresponding to the surface phase takes increasingly smaller wedges. As noted, eq 11 only holds for $L > 3^{1/3}$. For $1 < L < 3^{1/3}$ the entire $H-G$ phase diagram consists of the surface phase. This occurs because the lamellar spacing can only be λ or 2λ. For large L_b a spacing of 2λ is chosen because this is closest to the natural bulk spacing. For much smaller L_b, i.e., $L < 3^{1/3}$, the value of λ is closer to the natural spacing, and the stretched phase (of spacing 2λ) is never favored.

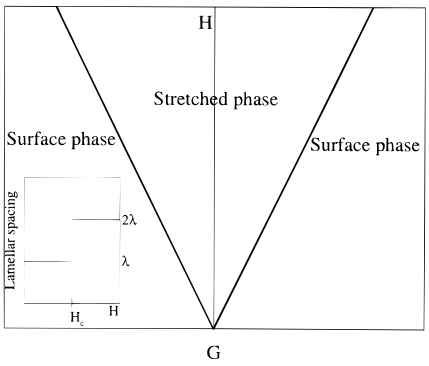

Figure 3. Phase diagram for the four-stripe model in the $H-G$ plane for a particular value of L such that $L > 3^{1/2}$. In this diagram we include the case $G < 0$, which corresponds to C stripes preferring A blocks and D stripes preferring B blocks. Note that, as expected, the phase diagram is symmetrical about $G = 0$. The inset shows the lamellar spacing as a function of H. Note the discontinuous jump at $H = H_c$.

In summary, there are two possible phases that may appear in the four stripe model, a surface phase that attempts to minimize the surface−diblock potential and a stretched phase that attempts to obtain the natural bulk spacing. Competition between these two effects yields a phase diagram as in Figure 3, where the phase transition occurs on a line through the origin in the $H-G$ plane. That the phase transition occurs on a line through the origin is a feature that appears in any n-stripe model.

2.2 Six-Stripe Model. Next we consider a system composed of three C stripes and three D stripes. Since this system is slightly larger and more complicated than the four-stripe system, it is able to show an additional phase to the two we have seen above. The three distinct phases that occur in the system are (Figure 4) (i) A surface phase with six equal lamellae of spacing λ, (ii) a stretched phase with two equal lamellae of spacing $6\lambda/2 = 3\lambda$, and (iii) an incommensurate phase, which is not locked into the surface−diblock potential, with four not neccessarily equal lamellae of average spacing $6\lambda/4 = 1.5\lambda$.

Note that we never see phases with odd numbers of lamellae. Presumably this is because the periodic boundary conditions impose an extra unfavorable AB interface in comparison with the even lamellae system and because the system is so small that such losses cannot be compensated for sufficiently. In larger stripe systems there is no reason to expect that we should not observe odd numbers of lamellae.

The appearance of the incommensurate phase makes the phase diagram more complex than for the previous case. This incommensurate phase and phases such as it feature strongly in systems with more than four stripes. To analyze the system, as before, we write the free energy corresponding to the three phases.

The first phase is the surface phase with free energy

$$F_{surf} = 6h\gamma_{AB}\left[\frac{\lambda^3}{2L_b^3} + 1\right] + 3\lambda[\gamma_{AD} + \gamma_{BC}] \qquad (12)$$

The second phase is the stretched phase. In contrast to the four stripe system, this phase is not a floating phase in that the position of the diblocks (specified by the x_i's) actually changes the free energy. The diblocks

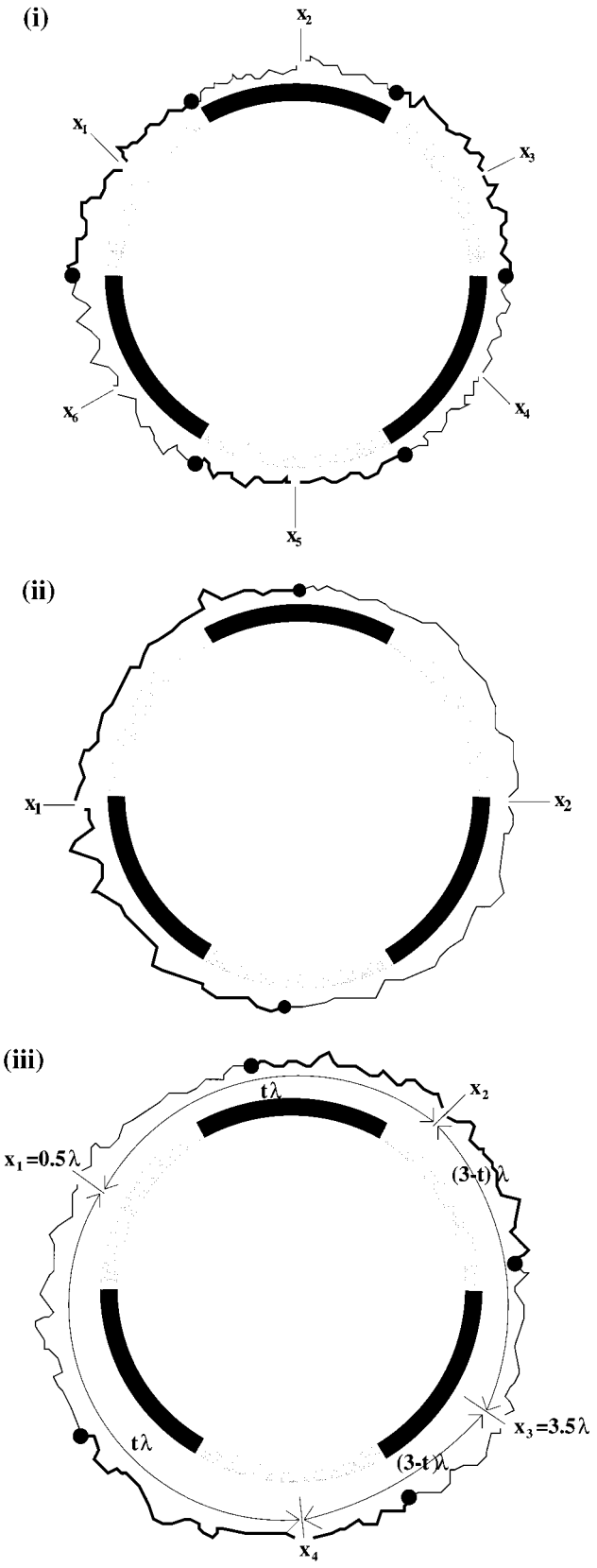

Figure 4. Three possible diblock configurations for the six-stripe model: (i) the surface phase with lamella spacing λ; (ii) the stretched phase with lamella spacing 3 λ; (iii) the incommensurate phase with diblock lengths ($t\lambda$, $(3 - t)\lambda$, $(3 - t)\lambda$, $t\lambda$). The same labeling scheme for stripes and A and B blocks as in Figure 2 applies here.

choose their positions in order to minimize this free energy. The free energy of this phase, Figure 4(ii), for the equilibrium x_i's is then then given by

$$F_{\text{stretch}} = 2h\gamma_{AB}\left[\frac{27\lambda^3}{2L_b{}^3} + 1\right] + \lambda[\gamma_{AC} + 2\gamma_{AD} + 2\gamma_{BC} + \gamma_{BD}] \quad (13)$$

The third phase that occurs is the incommensurate phase, with average lamellar spacing 1.5λ. In this phase the lamellae are not neccessarily of equal spacing and the free energy is then a function of the x_i's. From our numerical procedure we have observed that the incommensurate phase has the general configuration shown in Figure 4(iii), where x_1 and x_3 are always fixed at 0.5λ and 3.5λ, respectively. The x_2 and x_4 values vary such that $x_2 - x_1 = x_4 - x_1$, where both distances here are the shorter of the two possible distances in our system with periodic boundary conditions. Making this observation allows us to express the free energy simply as a function of one extra variable $t \equiv x_2 - x_1$, such that $3/2 \leq t \leq 2$. The free energy of the incommensurate phase is then

$$F_{\text{inc}} = 2h\gamma_{AB}\left[\frac{\lambda^3}{2L_b{}^3}(t^3 + (3 - t)^3) + 2\right] + 3\lambda[\gamma_{AC} + \gamma_{BD}] - \lambda t\Delta\gamma \quad (14)$$

The value of $t = {}^3/_2$ corresponds to all lamellar layers having equal spacing. When $t = 2$ we have two lamellae of spacing 2λ and two lamellae of spacing λ. The actual phase that appears in the system for any values of the variables h, γ_{AB}, and the surface−diblock interfacial energies is given by the minimum free energy of the above three phases.

It is clear that F_{inc} must be minimized with respect to our position variable, t, for any point in the H−G plane. Doing this we obtain the minimum free energy for this phase at

$$t_{\text{min}} = \frac{3}{2} + \frac{\lambda\Delta\gamma}{18\gamma_{AB}h}\left(\frac{L_b}{\lambda}\right)^3 = \frac{3}{2} + \frac{G}{18H} \quad (15)$$

Since t_{min} appears only as a function of G/H, the minimum free energy occurs on lines passing through the origin, with varying slope. As long as $H/G > 1/9$, the distance through which the diblocks are stretched corresponding to these lines are $t_{\text{min}}\lambda$, $(3 - t_{\text{min}})\lambda$, $(3 - t_{\text{min}})\lambda$, $t_{\text{min}}\lambda$. Note the corresponding lamellar spacings are $t_{\text{min}}\lambda$, ${}^3/_2\lambda$, $(3 - t_{\text{min}})\lambda$, and ${}^3/_2\lambda$. When $H/G \leq 1/9$, there is only one value of t ($t = 2$) corresponding to the minimum F_{inc}. Thus the incommensurate phase now has diblocks stretched through 2λ, λ, λ, 2λ, and corresponding lamellar spacings 2λ, ${}^3/_2\lambda$, λ, and ${}^3/_2\lambda$. The free energy of the incommensurate phase for this minimum value of t is then

$$F_{\text{inc}} = h\gamma_{AB}\left[\frac{27}{4}\left(\frac{\lambda}{L_b}\right)^3 + \left(\frac{9\lambda}{2\gamma_{AB}}\right)^2\left(\frac{L_b}{\lambda}\right)^3\left(\frac{\Delta\gamma}{h}\right)^2 + 4\right] - \lambda\Delta\gamma\left[\frac{3}{2} + \frac{\lambda}{18\gamma_{AB}}\left(\frac{L_b}{\lambda}\right)^3\left(\frac{\Delta\gamma}{h}\right)\right] + 3\lambda(\gamma_{AC} + \gamma_{BD}) \quad (16)$$

To construct the phase diagram, we need to compare the three free energies, eqs 12, 13, and 16, over a range of h and $\Delta\gamma$ for fixed bulk spacing L_b. This is algebra-

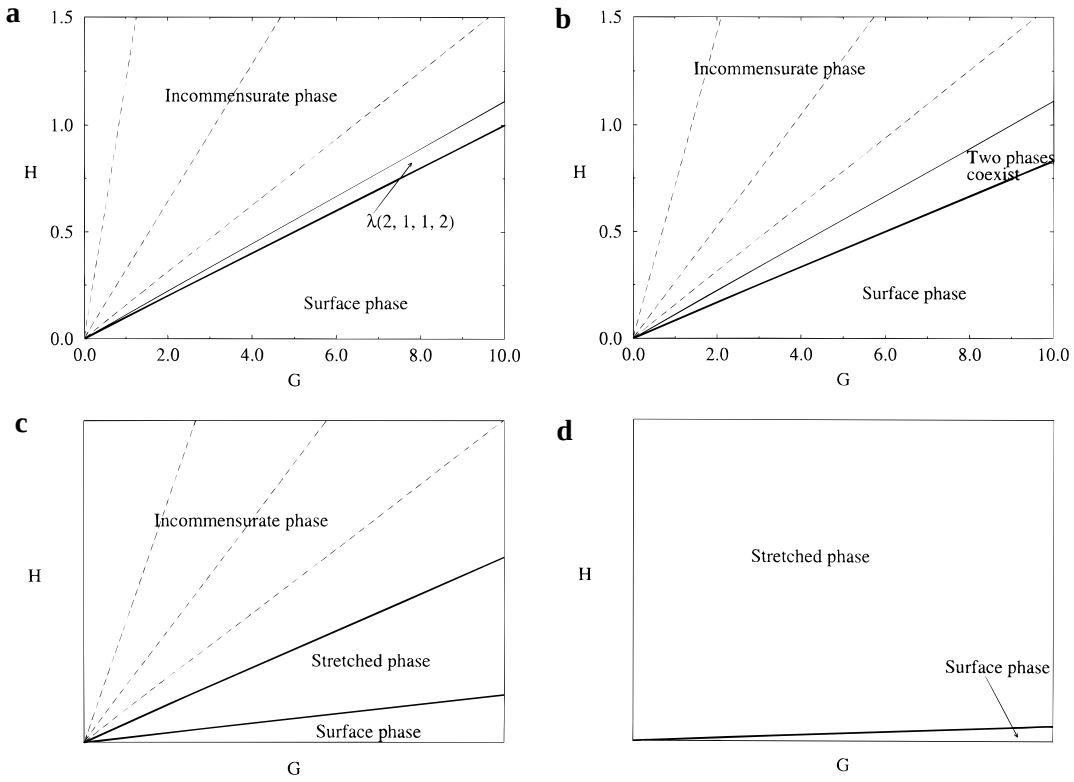

Figure 5. Phase diagram for the six-stripe model in the $H-G$ plane for (a) $L = 2$, (b) $L = L^{c} = 9^{1/3}$, (c) $L^{c} < L < L^{d}$ ($L^{d} = 3^{4/3}/2$), and (d) $L > L^{d}$. In (a) the wedge bounded by the bold line and the undashed line is where the incommensurate phase exists and has spacing $(2, 1, 1, 2)\lambda$. In (b) the incommensurate and stretched phases coexist in this wedge, while on the bold line all three phases coexist. See text for further explanations.

ically complicated, and we thus place the arguments in the Appendix. Here we present the results for the phase diagram.

Again we plot the phase diagrams, with respect to the dimensionless variables, in the form H versus G for fixed L. We first discuss the case where the bulk lamellar spacing is small, i.e., $L < 9^{1/3}$. Figure 5a shows a typical example of this when $L = 2$. In this case, near $H = 0$ we find a surface phase with all the lamellae having equal spacing λ. This is as expected—for very thin films the surface will always dominate and the diblocks will become locked into the surface. For slightly larger thicknesses $H > G/10$, an incommensurate phase appears with two lamellae of spacing λ and two lamellae of spacing 2λ. At larger thicknesses $H > G/9$, the spacings of the lamellae begin to change until for very thick films the spacings are all equal to 1.5λ. For these large thicknesses the lamellar spacings are not generally constant. However, along any straight line drawn from the origin the spacings will be constant. Examples of such lines are shown as dashed in the diagram.

At a critical value of the bulk spacing, $L = L^{c} = 9^{1/3}$, a stretched phase suddenly appears (Figure 5b). This phase coexists with the incommensurate phase over a range of thicknesses H; i.e., in the wedge shown in Figure 5b the stretched and incommensurate phases have equal free energies. For this value of L we again get a surface phase for very thin films and an incommensurate phase for thicker films.

For films with a slightly larger value of L again (Figure 5c), we obtain a surface phase for small thicknesses followed by a stretched phase for larger thicknesses $H > G/4(L^{3} - 6)$. At larger thicknesses still there is a transition from the stretched to the incommensurate phase and the incommensurate phase persists for very thick films.

For films with large values of the natural lamellae spacing, i.e., $L > 3^{4/3}/2$ the incommensurate phase completely dissappears and we have only a surface phase for thin films and a stretched phase for thicker films (Figure 5d).

The existence of the stretched phase seen in the four- and six-striped systems is in part an artifact of having a system of finite size. In general, for a very large system the stretched phase, i.e., one with only two lamellae, will never exist, because only two lamellae would have to span the whole system. The general behavior for these larger systems is thus more typically like that seen in Figure 5a, where at small thicknesses we find a surface phase, and at larger thicknesses we find one or more incommensurate phases. At small thicknesses the surface effects dominate, while for larger thicknesses the spacing chosen is close to the bulk spacing.

3. General Features and Numerical Extension

Let us discuss some of the general features of these diblock–stripe systems; features that should be observable in larger stripe systems and real experimental systems. As has been mentioned, we only consider systems where $L_b \geq \lambda$. In the case that $L_b < \lambda$ there are a number of different possible configurations that can occur. If L_b is close to λ the minimum energy configuration may be one where the diblocks are in a similar configuration to the surface phase but are actually tilted at an angle θ to the surface, where θ is given by $\cos\theta = L_b/\lambda$. By taking up this configuration, the diblocks not only minimize their bulk energy, i.e.,

their spacing is L_b, but they also minimize the surface−diblock energy since they are aligned with the stripes. In the case where L_b is much smaller than λ, the diblocks cannot "feel" the surface potential; i.e., this is similar to the case of placing diblocks on a homogeneous surface. In this case the orientation of the diblocks, i.e., either parallel or perpendicular to the surface, is determined by whether h or $2n\lambda$ is closer to an integer multiple of L_b.[8] Another possiblility for $L_b < \lambda$ is that the surface undulates.[3] We have briefly mentioned here the various possibilities for the case $L_b < \lambda$, a detailed investigation of this case is beyond the scope of the present study and is left to future work.

For $L \geq 1$ and fixed, the L versus G phase diagram will have the following form. For small thicknesses, i.e., H small, a surface phase will appear where the lamellae follow the surface exactly. This phase changes to an incommensurate phase at larger thicknesses. The boundary between the surface and incommensurate phases is always a straight line passing through the origin. In the incommensurate phase regime there will often be a large number of incommensurate phases. The surface and incommensurate phases have two main differences. The first is that in the surface phase the lamellar positions are locked into the stripe positions, whereas in the incommensurate phases this is never the case. The second difference is that in the surface phase the lamellae are all of equal spacing. In the incommensurate phases the lamellae are often of unequal spacing. How the lamellar spacings vary depends on the ratio of H/G. On lines passing through the origin with constant slope (H/G = constant), the lamellar spacings do not vary. As H/G becomes smaller, the lamellar spacings become more nonuniform. For large systems the stretched phase, which we found in the four- and six-stripe system will never be observed for experimentally realizable values of L_b.

Phase transitions from a surface to an incommensurate phase, a surface to a stretched phase, or an incommensurate to a stretched phase occur on lines passing through the origin. This is because the boundary lines between the phases are always of the form

$$\rho\frac{h_c\gamma_{AB}}{\lambda\Delta\gamma}f(\lambda/L_b) = 1 \quad \text{or} \quad \xi\frac{H}{G}f(L) = 1 \qquad (17)$$

where f is some function of L, and ρ and ξ are numerical constants. The term $wh_c\gamma_{AB}$ is the energy of an AB interface, where w is the length in the y direction. The term $w\lambda\Delta\gamma$ arises from the energy difference between the surface and different diblocks. The term in λ/L_b arises from the stretching of the diblocks. The expression (17) is thus a balance between the surface interaction and the bulk free energy.

These are all first-order transitions, as the lamellar spacings change discontinuously at these phase transitions. As L increases, the wedge corresponding to the surface phase, adjacent to the G-axis, takes up smaller and smaller regions. A general feature of these systems is that a new incommensurate phase will generally first appear on the phase transition line between the other two phases. As L increases, the wedge correponding to this new incommensurate phase will separate the other two phases and will grow in size.

We would like to see if our general conclusions on the features of the phase diagram of the diblock−stripe model hold for systems with larger numbers of stripes. As well, we might expect other, more novel, phases to appear in larger systems. For example, it may be that the diblocks arrange themselves in an inverted configuration, i.e., AB, AB. Exact analysis for larger systems becomes difficult in part because the number of possible equilibrium states becomes very large. Another difficulty that arises is that the description of many of these equilibrium states requires a large number of variables. Thus we saw in the six-stripe system that a new variable t was needed to describe the incommensurate phase. In systems with many stripes, many variables of this kind are needed and the exact expressions for the free energy rapidly become very complicated. Thus we must analyze these larger systems computationally. Consider a system of $2n$ stripes in total. To find the equilibrium state for this system, we need to minimize over many variables. We need to minimize over n_l, the number of lamellar layers, and also over the positions of each AB interface, i.e., the x_i's. We first choose a n_l and then use eq 7 to determine the free energy of the possible configurations of the diblocks. In our numerical procedure we allocate each x_i to a stripe (at random) and then minimize the resulting configurations free energy, with respect to the x_i's. The x_i's are only allowed to vary in the interval of the stripe to which they have been allocated. After minimizing over the x_i's we need to minimize over n_l.

The total number of possible configurations of such a system is of the order of $n_l(2n)^{n_l}$. Clearly, even if n and n_l are order 10, this means there will be an enormous number of possible configurations to analyze. Furthermore, the above procedure must be carried out for all possible numbers of lamellae from 2 to roughly n, to obtain the minimum free energy of the system. Last, we note the above procedure when completed will give just one point in the total (G, H, L) phase diagram.

It would obviously be desirable to analyze systems of the order of 100 or 1000 stripes. However, from our discussion above this is impossible. On the other hand we would like to obtain the features of a large system. To obtain a balance between these two sets of constraints, we have decided to carry out our numerical analysis in the following manner. We select a system of 20 stripes. All possible configurations are not analyzed. Instead we select a random subset of possible configurations. In this subset we include those configurations corresponding to equally spaced lamellar layers, since we know they must exist near the H- and G-axes. We then obtain the minimum free energy of these possible configurations. Even though we might not necessarily have the configuration corresponding to the minimum possible free energy, general features of the system should become apparent. For the 20-stripe system the possible incommensurate phases are those with 3, 4, 5, 6, ..., 19 lamellar layers.

We have studied this system in some detail and verified that the general features outlined above, and also those which appear in the four- and six-stripe models, are found here. However, for the sake of brevity, we present here only two representative slices of the total (G, H, L) phase diagram. Following this we shall comment on some of the more unusual phases we observed in our study and discuss some of their properties. Note that in the following discussion it is more convenient to give our results in terms of the distance through which a diblock is stretched, i.e., ($x_{i+1} - x_i$) rather than the corresponding lamellar spacing.

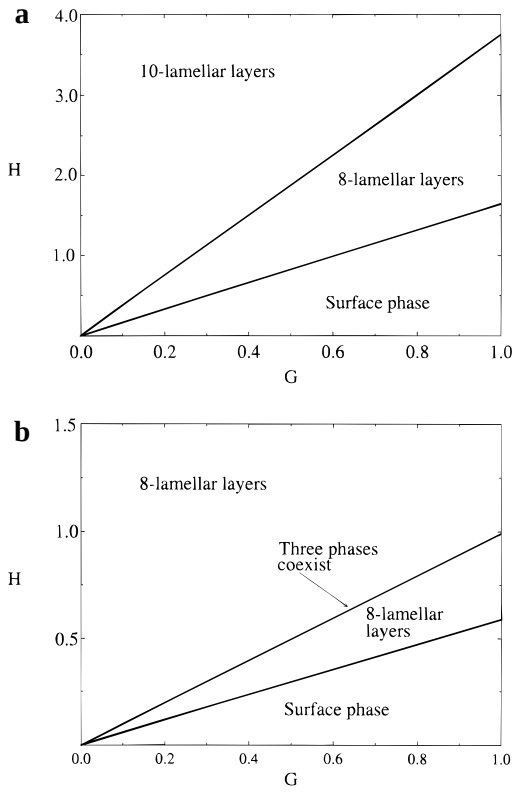

Figure 6. Phase diagram for the 20 stripe model in the $H-G$ plane for (a) $L = 2.201$ and (b) $L = 2.771$.

Figure 6a shows the phase diagram for the twenty-stripe model for the value of $L = 2.201$. For this value of L we find a surface phase with twenty lamellar layers exists close to the G-axis. As we increase the thickness of the diblock film, at constant G, we find at thicknesses of $H > 1.649G$ an incommensurate phase with eight lamellar layers appears. At the phase transition line the lengths of the diblocks in the phase with eight lamellar layers are (2.503, 2.994, 2.503, 2.295, 2.295, 2.821, 2.295, 2.295)λ. Note that these lengths are not all the same. As one further increases the film thickness, this eight-lamellar phase continuously changes its lamellar spacing, in much the same way as the incommensurate phase did in the six-stripe model. Once again we verified that on lines through the origin these spacings did not vary. On further increase of the film thickness we observe the appearance of a phase with 10 lamellar layers. This we observed numerically to occur at $H = 3.75G$. At this phase transition line the lengths through which the diblocks are stretched in the phase with 10 lamellae were found to be (2.009, 2.009, 2.009, 2.009, 2.009, 2.009, 2.564, 2.061, 1.312, 2.009)λ. Note in this case most of the lengths are close to 2.0, except for one which is much greater than 2.0λ (2.564λ) and one much less than 2.0λ (1.312λ). Increasing the film thickness further results in this ten-lamellar phase varying its spacings until for very thick films we observe ten equally spaced lamellae of spacing 2λ.

Next we consider the phase diagram corresponding to the value $L = 2.771$. This value is a special value because it the first value of L at which a phase with six-lamellar layers appears. As in the six stripe model we observe that it appears on the same line as the phase transition between two other phases. Figure 6b displays the phase diagram for $L = 2.771$. As before close to the G-axis we find the surface phase. Increasing the film thickness, at constant G results in a phase with eight lamellae appearing for $H > 0.55G$. This phase is interesting because it has inverted lamellar configurations in it. We find that the diblocks are stretched through lengths (2.885, 1.779, 1.779, 4.000, 2.000, 2.000, 2.442, 3.115)λ in the pattern AB, BA, AB, BA, AB, AB, AB, BA. Note that this eight-lamellar phase is totally unrelated to the eight-lamellar phase mentioned previously, i.e., for $L = 2.201$. A further increase in H results in various other eight-lamellar phases appearing. At $H = 0.99G$ we observe that three different phases coexist on the same line. These three phases are (i) an eight-lamellar phase with lengths (2.399, 3.202, 2.399, 2.231, 2.231, 3.076, 2.231, 2.231)λ. This phase is related to the eight-lamellar phase we observed above for $L = 2.201$, (ii) an eight-lamellar phase with lengths (2.953, 1.969, 1.969, 3.586, 2.000, 2.238, 2.238, 3.047)λ, and (iii) a six-lamellar phase with lengths (3.754, 3.508, 2.984, 3.016, 2.984, 3.754)λ. For very thick films we observe a phase with eight equal lamellae of equal spacings of 2.5λ.

The above two phase diagrams are fairly representative of our results. We have studied systems with much larger L and observed other incommensurate phases as well as the stretched phase. One point to be made about this study is that we cannot be absolutely certain that the incommensurate phases we have seen are necessarily the lowest free energy states. However, as in an experimental system, the lowest free energy state may in fact not be the one the system is observed in because the system may become trapped in local minima, rather than finding the global minima.

One of the interesting observations of this study has been the appearance of inverted configurations. To be relatively sure that such states were close to the lowest free energy state, we decided to let our computational program run for an extended period, so that as many as possible random configurations could be sampled. We did this for the particular set of values $L = 2.808$ and $H/G = 0.6$ and found the lowest free energy state to be one with seven lamellar layers. For this configuration the diblocks are stretched through lengths (2.429, 2.429, 3.141, 2.858, 3.141, 2.858, 3.141)λ, in the pattern BA, BA, AB, BA, AB, BA, AB. Besides the appearance of an inverted pattern, this configuration is novel because we find an odd number of lamellae, i.e., seven. In the four- and six-stripe models, odd numbers of lamallae were never seen, presumably because the system was so small.

4. Relationship to Frenkel−Kontorowa Model

The Frenkel−Kontorowa (FK) model[13−15] provides the simplest, realistic model for adsorption of atoms onto a one-dimensional periodic surface. The adsorbed atoms are at position x_i and are treated as a harmonic chain with equilibrium separation b. The surface is a one-dimensional periodic lattice with periodic spacing c. The energy in the FK model is then given by

$$F = \sum_i \left\{ \frac{1}{2} K(x_{i+1} - x_i - b)^2 + V(x_i) \right\} \qquad (18)$$

where K is a constant depending on the interatomic interactions and $V(x_i)$ is the potential energy betweeen the surface and the atom at x_i. Generally, the potential energy $V(x_i)$ is taken to be a sinusoidal function, i.e.,

$V(x) = -V_0 \cos(2\pi x/c)$. When the potential term is dominant, this results in atoms locking into the surface potential; i.e., atoms are positioned at the minima of $V(x_i)$. This state is called a *commensurate* state. On the other hand, when the potential $V(x_i)$ is zero, the atoms will try and remain b units apart, irrespective of the surface. This is a floating state, since the x_i's are independent of the surface. The floating phase is *incommensurate*. In the FK model for the commensurate state the atoms are in general a rational multiple of c units apart.

On a qualitative level there seems to be a fair deal of similarity between the FK model and our model. Here we do not consider the possibility of inverted (i.e., AB, AB) configurations. In this case the variable part of the bulk free energy per unit length w in our model can be put in the form $(K_1/2)(x_{i+1} - x_i - L_b)^2 + \ldots$ where $K_1 = 3\kappa h L_b$. This is the same as the elastic term in the FK model. However, the potential terms in the two models are not exactly the same.

To discuss this in more detail, it is mathematically more convenient to introduce a sinusoidal potential for the surface−diblock potential, rather than the square well potential used so far. Thus we define

$$\gamma_{AS} = \gamma_{A0} + \alpha_A \cos\left(\frac{\pi}{\lambda}x\right)$$

$$\gamma_{BS} = \gamma_{B0} + \alpha_B \cos\left(\frac{\pi}{\lambda}x\right) \qquad (19)$$

and note that the origin of the x-coordinate is at the center of the first C stripe. In eq 19 γ_{AS} and γ_{BS} refer to the interfacial tensions between the surface and A and B blocks, respectively. These interfacial tensions are broken up into a constant part and a variable part, which has sinusoidal variation. The constants α_A and α_B are not equal, and so the sign of $\alpha_A - \alpha_B$ defines which block prefers which stripe. In accordance with previous sections we thus assume $\alpha_A - \alpha_B > 0$ so that in the first, third, fifth, ... stripes (i.e., C stripes) the B blocks are preferred, while in the second, fourth, sixth, ... stripes (i.e., D stripes) the A blocks are preferred. The surface energy per unit length w is then obtained by summing eq 19 over the entire striped surface. Doing this and combining with the stretching energy, one obtains

$$F_T = \sum_i \left\{ \frac{1}{2}K_1(x_{i+1} - x_i - L_b)^2 + \frac{(\alpha_A - \alpha_B)\lambda}{\pi}(-1)^i \sin\left[\frac{\pi}{\lambda}\left(\frac{x_{i+1} + x_i}{2}\right)\right]\right\} \qquad (20)$$

ignoring constant terms in the free energy. The difference between eqs 18 and 20 lies in the fact that the sinusoidal dependence in eq 20 is not solely a function of x_i but rather a function of x_i and x_{i+1}. Thus this term may not be decoupled as in eq 18. If we consider a particle as the end of a BAAB repeat unit, then, in contrast to the FK model, where particles only sample the potential at x_i, in our model the particle samples the potential in the neigbourhood about itself. As a consequence of this there exists only one commensurate state in our model—the surface phase. Placing particles at any other integer multiple of the surface spacing will not be energy efficient because the blocks will not be aligned with their preferred stripes; i.e., A blocks will be forced to stretch across unfavorable C regions. Thus there does not seem to be an exact mapping between the FK model 18 and our model (eq 7). However, for the case where the bulk lamellar spacing L_b is close to λ, there does exist an analogy between the two models. We shall discuss this below.

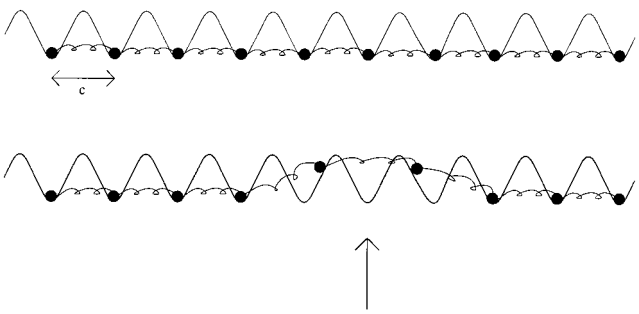

Figure 7. In the top diagram we have a a commensurate state with particles placed a distance c apart, while in the bottom diagram we have an incommensurate phase with a positive discommensuration, where springs are stretched relative to the surface lattice spacing. The arrow marks the discommensuration.

In the FK model there can be a transition from a commensurate state to an incommensurate state, by the introduction of a small *discommensuration*, or defect, in the commensurate state (see Figure 7). Generally, the creation of a defect requires energy, and so there exist finite intervals about rational multiples of c where the commensurate state exists. The commensurate−incommensurate (CI) transition in the FK model is second-order.

Let us discuss this CI transition in the context of the diblock−stripe model. As mentioned above, the only commensurate state that exists in this model is the surface phase with spacing λ. Thus we only consider $b/c = 1$. Now when L_b is close to λ, but not exactly the same, there exists a mismatch between the two potential scales. As the surface potential varies, there can therefore be a CI transition. We restrict ourselves to the limit where $\delta = L_b - \lambda$ is small (i.e., $\delta \ll \lambda$ and remember $\delta > 0$, since $L_b > \lambda$) and there are weak surface potentials (i.e., $\alpha_A - \alpha_B \ll K_1 \lambda$). In this limit the index i can be treated as a continuous variable. The commensurate state has $x_i = i\lambda$, while the incommensurate state has x_i's with small deviations $\phi(i)$ from $i\lambda$ so that in the incommensurate state $x_i = i\lambda + \phi(i)$. Substituting this expression for x_i into eq 20 and making the change from a sum to an integral, since i is now a continuous variable, we obtain

$$F_T = \int \left[\frac{1}{2}K_1\left(\frac{d\phi}{di} - \delta\right)^2 + \frac{(\alpha_A - \alpha_B)\lambda}{\pi}\cos\left(\frac{\pi}{\lambda}\phi(i)\right)\right] di \qquad (21)$$

To obtain this equation we have made the approximation $[\phi(i) + \phi(i+1)]/2 \approx \phi(i)$, which is valid for small ϕ. This expression for F_T has precisely the same form of the energy in the continuum limit of the FK model.[13] Thus a formal relationship is now established between the two models in the limit of small δ and weak surface potentials. Results from eq 21 show that there exists a critical value of δ below which only the commensurate state exists. This critical value is given by

$$\delta_c = (2\lambda)^{-1}\int_0^{2\lambda} d\phi \left[2\frac{(\alpha_A - \alpha_B)\lambda}{K_1\pi}\sin^2\left(\frac{\pi\phi}{2\lambda}\right)\right]^{1/2} = \frac{4}{\pi}\left[\frac{(\alpha_A - \alpha_B)}{\pi K_1}\right]^{1/2} \quad (22)$$

The incommensurate phase that appears is one where the diblocks in the discommensuration are slightly stretched compared to the rest. This occurs when $\delta > \delta_c$. For $\delta < \delta_c$ the commensurate state exists. The distance between discommensurations is $D \propto \ln([\delta - \delta_c]^{-1})$. When $\delta \leq \delta_c$ the discommensurations are infinitely far apart;i.e., the diblocks are in the surface phase. As δ increases slightly above δ_c, discommensurations appear and are spaced D apart. A further increase in δ causes this spacing to decrease, and so more discommensurations must appear. The difference between the average particle spacing, $\langle L\rangle$, and 2λ can also be shown to be proportional to $1/\ln([\delta - \delta_c]^{-1})$. For $\delta < \delta_c$ the particles have equal spacing of 2λ, so that $\langle L\rangle - 2\lambda = 0$. For δ sligthly larger than δ_c, this difference increases continuously, so that at $\delta = \delta_c$ there must be a second-order CI transition.

5. Conclusions

The present study is concerned with the equilibrium properties of a symmetrical diblock copolymer melt on a heterogeneous, striped surface. The A and B blocks have different surface energies with each of the C and D stripes. As a result there exists a competition between the bulk lamellar spacing of the diblocks, L_b and the width of the stripes, λ. For systems where the surface energies are most important we find the lamellae align commensurate with the surface stripes. We call such a phase the surface phase. When the diblock-surface energies are less important, the lamellae do not necessarily align with the surface stripes. Such phases are incommensurate. The incommensurate phase may have lamellae with spacings not all the same. We have also observed the existence of inverted lamellae, i.e., an AB, AB pattern rather than the usual AB, BA pattern.

It is interesting to note that recent experimental studies[11] of diblock−stripe systems have observed something similar to a surface phase. In these experimental studies[11] only one diblock melt thickness has been studied. The lamellae were observed to align perpendicular to the striped surface, as we assume. It was also observed the lamellae aligned commensurate with the stripes, i.e., the surface phase. Most interestingly, this surface phase was observed even though the bulk lamellar spacing and stripe width differed by a significant factor. Further experimental observation of the incommensurate phases that we predict have not been seen, presumably because only one diblock melt thickness has been used. Nevertheless, these experimental results are extremely encouraging.

In the special limit where $L_b \approx \lambda$ and the surface potentials are weak, we have determined an exact mapping between the diblock−stripe model and the FK model[13] of solid-state physics. When L_b differs slightly from λ, we find small discommensurations or defects appear in the surface phase. These defects will be manifested as lamellae with spacing slightly larger than λ and occur periodically across the surface.

The study presented here is the simplest approximation to the diblock−stripe system. In the future we intend to investigate when parallel alignment of the lamellae will occur. Also we intend to relax the constraint that the top air/copolymer interface is flat.[19,20] Assuming this surface has roughness introduces an extra competition into the system, i.e., the air/copolymer surface energy.

Appendix

In this Appendix we consider the algebraic manipulation of the three free energies, eqs 12−14, to determine the phase diagram of the six-stripe model. In a manner analogous to the analysis of the four-stripe model, to determine which phase exists, we define the differences $\Delta F_1 = (F_{int} - F_{surf})/(\kappa\lambda^4)$, $\Delta F_2 = (F_{surf} - F_{stretch})/(\kappa\lambda^4)$, and $\Delta F_3 = (F_{stretch} - F_{int})/(\kappa\lambda^4)$. These are given by

$$\Delta F_1 = H[(t^3 + (3-t)^3 - 3) - 2L^3] + (3-t)G \quad (A1)$$

$$\Delta F_2 = -4H[6 - L^3] - G \quad (A2)$$

$$\Delta F_3 = H[(27 - t^3 - (3-t)^3) - 2L^3] + (t-2)G \quad (A3)$$

Note that we find it easier to manipulate these formulas in terms of t rather than eliminating this variable in favor of G/H via eq 15. It is clear these functions are only dependent on the set of variables (G, H, L). Thus it is now possible to determine an appropriate phase diagram for the six-stripe system.

To do this, we obtain slices of the phase diagram in the $H-G$ plane, for various L. From before, we remember that for small values of L the surface phase takes up the entire phase diagram slice. For the six-stripe model this corresponds to $1 \leq L \leq (15/8)^{1/3}$. Initially, we consider the case corresponding to $L = 2$. For this value of L we would expect the surface and incommensurate phases to exist.

Now for $L = 2$, for small H, or large G, we would expect the surface phase to appear, while for large H, or small G, we would expect the incommensurate phase to appear. It may be shown that ΔF_1 is a decreasing function of H/G and for $H/G = 0$ this function is positive. In fact, this result holds for all $L > 2$ and we will have cause to use it later. The phase transition from the surface to incommensurate phase therefore occurs when $\Delta F_1 = 0$. This transition may either be to the configuration with diblock lengths 2λ and λ or the configuration with diblock lengths $t_{min}\lambda$ and $(3 - t_{min})\lambda$. By solving $\Delta F_1 = 0$ we find the phase transition from surface to incommensurate phase, with diblocks stretched through lengths λ and 2λ, occurs on the line

$$H_c = \frac{G}{2[L^3 - 3]} \quad (A4)$$

Remembering that we are considering $L = 2$, this simplifies to $H_c = G/10$. This line has a smaller gradient than the line where the diblocks with lengths $t_{min}\lambda$ and $(3 - t_{min})\lambda$ first appear. They appear when $H = G/9$. Finally, it is easy to show for this value of L that $F_{stretch}$ is always greater than F_{int} and F_{surf}.

On increasing the value of L, we would expect at some stage the stretched phase to appear. However, we first note that both eqs 15 and A4 hold in this region. Equation 15 is independent of L so the lamellar layers with spacings $t_{min}\lambda$, $^3/_2\lambda$, $(3 - t_{min})\lambda$, and $^3/_2\lambda$ occur on the same lines as L increases. Equation A4, on the other hand, is not independent of L, and in fact, the gradient of this line decreases as L increases. Thus the surface

phase, as in the four-stripe case, takes up smaller and smaller wedges as L increases. We now return to the question of when the stretched phase first appears. One may show that ΔF_2 is an increasing function of H/G. Thus for fixed G the stretched phase has lower free energy than the surface phase for $H > H_{sb}$ where H_{sb} denotes the value of H at which both phases have equal free energy. Furthermore, as L increases, H_{sb} decreases and for small L, H_{sb} is large. Now one may also show ΔF_3 is an increasing function of H/G. Hence for $H < H_{ib}$ the stretched phase has a lower free energy than the surface phase. Here H_{ib} denotes the value of H where both stretched and incommensurate states have equal energy. As L increases H_{ib} increases, and for small L, H_{ib} is also small. The result of these arguments implies the stretched phase must first appear when both $\Delta F_2 = 0$ and $\Delta F_3 = 0$. This implies all three free energies are equal and this may only occur on the phase transition line between surface and incommensurate phases. Since we know the surface to incommensurate transition only occurs for $t = 2$, this gives an additional constraint. Solving for $\Delta F_3 = 0$ gives $\Delta F_3 = 2H[9 - L^3] = 0$. Thus the critical value of L when the stretched phase first appears is

$$L^c = 9^{1/3} \tag{A5}$$

and this occurs on the line given by solving $\Delta F_2 = 0$ or eq A4. Substituting the value of L^c into eq A4 we find

$$H_c = \frac{G}{12} \tag{A6}$$

For $L < L^c$ only surface and incommensurate phases exist in a manner analogous to that of the $L = 9^{1/3}$ case, except the phase transition line changes. When $L = L^c$ all three phases coexist on the line given by eq A6. Since the condition that $\Delta F_3 = 0$ is independent of H/G, in the wedge up to the line $H = G/9$, both stretched and incommensurate phases coexist. For $H > G/9$ the incommensurate phase with lamellar spacings $(3 - t_{min})\lambda$, $^3/_2\lambda$, $t_{min}\lambda$, and $^3/_2\lambda$ exists.

For $L > L^c$ the stretched phase appears between the surface phase and incommensurate phases. The surface phase appears in the wedge adjacent to the G-axis, and the incommensurate phase appears in the wedge adjacent to the H-axis. The phase transition from the surface phase to the stretched phase occurs when $\Delta F_2 = 0$ or when

$$H_{sb} = \frac{G}{4[L^3 - 6]} \tag{A7}$$

As L increases, the denominator in eq A7 increases and so the slope of the line decreases. Thus the wedge that the surface phase is confined to becomes smaller and smaller.

Now at what point does the phase transition from the stretched phase to the incommensurate phase occur? From eq A3 it is clear ΔF_3 is a decreasing function of L. Furthermore, it is also possible to show ΔF_3 is an increasing function of H/G. Thus as L increases, the phase transition from the stretched to incommensurate phase must occur deeper in the incommensurate region. That is, the phase transition must occur on lines of greater slope as L increases. We have already seen that in the region of the incommensurate phase the actual configuratiosn that occur are lamellar layers with spacing $(3 - t_{min})\lambda$, $^3/_2\lambda$, $t_{min}\lambda$, and $^3/_2\lambda$ which appear on lines going through the origin. By solving $\Delta F_3 = 0$ together with eq 15, we find the value of t at which the stretched to incommensurate phase transition occurs is given by

$$t_{bi} = 2 - \sqrt{2L^3/9 - 2} \tag{A8}$$

At $L = 9^{1/3}$ this corresponds to $t_{bi} = 2$, as we found before. As L increases, t_{bi} decreases. The minimum value t_{bi} can decrease to is $^3/_2$, and this occurs on the line $G = 0$. By equating the square root in eq A8 to $^1/_2$, we find the incommensurate phase disappears when $L > L^d = 3^{4/3}/2$. The equation of the phase transition line between stretched and incommensurate phases is then given by

$$H_{bi} = \frac{G}{18[2 - \sqrt{2L^3/9 - 2}]} \tag{A9}$$

Acknowledgment. G.G.P. and D.R.M.W. acknowledge support from an ARC large grant, and D.R.M.W. was funded by a QEII fellowship. They thank Liu et al. for useful discussions and for providing a copy of their preprint[11] prior to publication.

References and Notes

(1) Turner, M. S. *Phys. Rev. Lett.* **1992**, *69*, 1788.
(2) Turner, M. S.; Joanny, J.-F. *Macromolecules* **1992**, *25*, 6681.
(3) Williams, D. R. M. *Phys. Rev. Lett.* **1995**, *75*, 453.
(4) Kellogg, G. J.; Walton, D. G.; Mayes, A. M.; Lambooy, P.; Gallagher, P. D.; Satija, S. K. *Phys. Rev. Lett.* **1996**, *76*, 2503. Walton, D. G.; Kellogg, G. J.; Mayes, A. M.; Lambooy, P.; Russell, T. P. *Macromolecules* **1994**, *27*, 6225.
(5) Coulon, G.; Collin, B.; Ausserre, D.; Chatenay, D.; Russell, T. P. *J. Phys. (France)* **1990**, *51*, 2801.
(6) Coulon, G.; Collin, B.; Chatenay, D.; Gallot, Y. *J. Phys. II (France)* **1993**, *3*, 697.
(7) Coulon, G.; Russell, T. P.; Deline, V. R.; Green, P. F. *Macromolecules* **1989**, *22*, 2581. Anastasiadis, S. H.; Russell, T. P.; Satija, S. J.; Majkrzak, C. F. *Phys. Rev. Lett.* **1989**, *62*, 1852.
(8) Pickett, G. T.; Balazs, A. C. *Macromolecules* **1997**, *30*, 3097.
(9) Halperin, A.; Sommer, J. U.; Daoud, M. *Europhys. Lett.* **1995**, *29*, 297.
(10) Stocker W.; Beckmann J.; Stadler R.; Rabe J. *Macromolecules* **1996**, *29*, 7502.
(11) Liu, Y.; Rockford, L.; Russell, T. P.; Mansky, P.; Soong, S.; Yoon, M.; Mochrie, S. Submitted to *Nature*.
(12) Pereira, G. G.; Williams D. R. M. *Phys. Rev. Lett.* **1998**, *80*, 2849.
(13) Chaikin, P. M.; Lubensky, T. C. *Principles of condensed matter physics*; Cambridge University Press: Cambridge, U.K., 1995; p 601.
(14) Frenkel, Y. I.; Kontorowa, T. *Zh. Eksp. Teor. Fiz.* **1938**, *8*, 1340.
(15) Frank, F. C.; Van der Merwe, J. H. *Proc. R. Soc. London* **1948**, *198*, 205.
(16) Bates, F. S.; Fredrickson G. H. *Annu. Rev. Phys. Chem.* **1990**, *41*, 525.
(17) Helfand, R.; Wasserman, Z. R. *Macromolecules* **1976**, *9*, 879.
(18) Semenov, A. N. *Sov. Phys. JETP (Engl. Transl.)* **1985**, *61*, 733; *Zh. Eksp. Teor. Fiz.* **1985**, *88*, 1242.
(19) Petera, D.; Muthukumar, M. *J. Chem. Phys.* **1997**, *107*, 9640.
(20) Chen, H.; Chakrabarti, A. *J. Chem. Phys.* **1998**, *108*, 6897.

MA980244S